Charge Effects in the Transient Adsorption of Ionic Surfactants at Fluid Interfaces

C. A. MacLeod and C. J. Radke*

Department of Chemical Engineering, University of California Berkeley, Berkeley, California 94720

Received April 11, 1994. In Final Form: July 18, 1994[⊗]

A rigorous model is presented for diffusive transport of ionic surfactants to an adsorbing interface. The proposed model considers both the diffusion and migration of surfactant, counterions, and background electrolyte in the electric field that develops as the charged surfactant adsorbs at an interface. The transient electrical double-layer structure arising from specific adsorption of the surfactant is calculated by solving the coupled Nernst–Planck and Poisson equations in the bulk phase using a Frumkin constitutive relation for the interfacial boundary condition. The resulting transient double-layer model is valid over all time scales and for interfacial potentials and background electrolyte concentrations of any magnitude. Therefore, the proposed model is more general than previously derived "quasiequilibrium" models of ionic surfactant transport to the interface that require instantaneous equilibrium potentials in the double layer.[1-4] We compare results from the proposed ionic surfactant transport model to results from the standard Ward–Tordai model for nonionic surfactants adsorbing at a fluid/fluid interface. For low concentrations of strongly adsorbing surfactant, in the absence of background electrolyte, electrostatic effects decrease the equilibrium adsorption of surfactant by an order of magnitude. Correspondingly, the time required for equilibration of the interface is decreased. When the transient adsorption is scaled to eliminate differences due solely to different equilibrium adsorption, we discover that the rate of diffusion-limited transport of an ionic surfactant is decreased by an order of magnitude compared to that of an equivalent nonionic surfactant. Addition of nonadsorbing background electrolyte, increasing surfactant concentration, or weaker adsorption of surfactants decreases the electrostatic effects. A simple quasiequilibrium model that assumes a double layer in instantaneous equilibrium with an electroneutral bulk solution is also developed. Comparison of this quasiequilibrium model to the full transient model shows that, for a typical surfactant (e.g., sodium dodecyl sulfate) adsorbing at the water/air interface, differences between the full transient model and quasiequilibrium model occur only at times inaccessible to current dynamic surface tension techniques.

Introduction

Dynamic interfacial tension is a widely used tool for probing surfactant adsorption/desorption kinetics at deformable interfaces. After the interface is disturbed, the interfacial tension is measured as a function of time to monitor surfactant adsorption at the interface. Surfactant mass transfer in these experiments is described using some variation of the Ward–Tordai analysis of diffusion and adsorption at the interface.[5] An important area of considerable debate is the possible existence of kinetic barriers to surfactant adsorption over measurable time scales.[4,6-15] However, analysis of the entire real-time transient interfacial tensions of several small, nonionic surfactants[13,16,17] demonstrates sorption kinetics in which diffusion to the interface is the limiting transport resistance over all times measured.

For ionic surfactants, no such clear picture has emerged. The similarity of the physical structure (i.e., short hydrocarbon tail and small head group) of a typical ionic surfactant (e.g., sodium dodecyl sulfate (SDS)) to that of nonionic surfactants (e.g., 1-decanol) that exhibit fast local exchange between the solution and the interface suggests that ionic surfactants should exchange at similar rates. However, conflicting studies on SDS describe transport that is diffusion limited,[18] kinetic limited,[4,19] and mixed diffusion–kinetic.[10,11]

One apparent reason for the discrepancy in describing SDS transport is that no rigorous model exists for describing the bulk phase transport of an ionic surfactant near a surfactant-laden and, hence, charged interface. In the absence of such a model, the standard means of analyzing dynamic tensions of ionic surfactants is through the Ward–Tordai diffusion model using a classical Langmuir adsorption isotherm.[10,11,18,19] This type of analysis ignores the possible effects that electrostatic interactions have on both the equilibrium partitioning between the bulk and interface and the rate of transport to the interface.

Davies[20,21] presents an equilibrium adsorption isotherm for ionic surfactants that includes electrostatic effects, accounting for the interfacial charge and the resulting electrical double layer that exists near the interface. Borwanker and Wasan use the isotherm of Davies to consider the diffusion-limited transport of ionic surfactant to a double layer in local quasiequilibrium with surfactant in the adajcent bulk solution[4] and the kinetic-limited transport of an ionic surfactant to the interface.[22] Dukhin

[⊗] Abstract published in *Advance ACS Abstracts,* September 1, 1994.

(1) Dukhin, S. S.; Miller, R.; Kretzschmar, G. *Colloid Polym. Sci.* **1983**, *261*, 335.
(2) Dukhin, S. S.; Miller, R. *Colloid Polym. Sci.* **1991**, *269*, 923.
(3) Miller, R.; Dukhin, S. S.; Kretzschmar, G. *Colloid Polym. Sci.* **1985**, *263*, 420.
(4) Borwanker, R. P.; Wasan, D. T. *Chem. Eng. Sci.* **1986**, *41*, 199.
(5) Ward, A. F.; Tordai, L. *J. Chem. Phys.* **1946**, *14*, 453.
(6) Miller, R.; Lunkenheimer, K. *Colloid Polym. Sci.* **1986**, *264*, 357.
(7) Miller, R.; Schano, K. H. *Colloid Polym. Sci.* **1986**, *264*, 277.
(8) Miller, R. *Colloids Surf.* **1990**, *46*, 75.
(9) Miller, R.; Kretzschmar, G. *Adv. Colloid Interface Sci.* **1991**, *37*, 97.
(10) Bonfillon, A.; Langevin, D. *Langmuir* **1993**, *9*, 2172.
(11) Chang, C. H.; Francis, E. I. *Colloids Surf.* **1992**, *69*, 189.
(12) Fainerman, V. B. *Colloid J. U.S.S.R.* **1978**, *40*, 769.
(13) Lin, S. Y.; McKeigue, K.; Maldarelli, C. *Langmuir* **1991**, *7*, 1055.
(14) Ravera, F.; Liggieri, L.; Steinchen, A. *J. Colloid Interface Sci.* **1993**, *156*, 109.
(15) Tsonopoulos, C.; Newman, J.; Prausnitz, J. M. *Chem. Eng. Sci.* **1971**, *26*, 817.
(16) Lin, S. Y.; McKeigue, K.; Maldarelli, C. *AIChE J.* **1990**, *36*, 1785.
(17) MacLeod, C. A.; Radke, C. J. *J. Colloid Interface Sci.* **1994**, *166*, 73.
(18) Joos, P.; Fang, J. P.; Serrien, G. *J. Colloid Interface Sci.* **1992**, *15*, 144.
(19) Matuura, R.; Kimizuka, H.; Yatsunami, K. *Bull. Chem. Soc. Jpn.* **1959**, *32*, 404.
(20) Davies, J. T. *Proc. R. Soc. London* **1958**, *a245*, 417.
(21) Davies, J. T. *Proc. R. Soc. London* **1958**, *a245*, 429.

0743-7463/94/2410-3555$04.50/0

et al.[1-3] have developed a model describing the transport of charged surfactants through an electrical double-layer potential field that is always assumed to be at a local quasiequilibrium with the ion concentrations at the outer boundary of the double layer. The requirement of equilibrium concentrations and/or potential within the double layer limits quasiequilibrium models to long times (i.e., times greater than the ion transport within the double layer) and to cases where a large amount of indifferent electrolyte is present. Clearly, further consideration of ionic surfactant transport is advisable.

Here we present a model for transport of ionic surfactants that considers rigorously the effects of surfactant charge accumulation at an interface. The model considers the diffusion and migration of surfactant, counterions, and background electrolyte in the building electric field that develops as charged surfactant adsorbs at the interface. On the basis of a numerical scheme similar to that of Murphey et al.,[23] we develop solutions of the coupled Nernst–Planck and Poisson equations for combined diffusion–kinetic transport to an interface. We then examine the effect that charge has on the diffusion-limited transport of surfactant to an interface. We also propose a quasiequilibrium model similar to that of Borwanker and Wasan,[4] in which the entire electrical double layer (including surfactant) is assumed to be in instantaneous equilibrium with ion concentrations at the double-layer periphery. Finally, our proposed quasiequilibrium model is compared to the full transient double-layer model, and the implications of our results to dynamic surface tension measurements are discussed.

Theory

To describe the kinetics of surfactant adsorption, we focus on the case of surfactant diffusion through an unstirred, semi-infinite bulk aqueous solution followed by adsorption at a planar, stationary interface. As in the standard Ward–Tordai analysis,[5] we consider an interface that is initially totally depleted of surfactant and is in contact with a uniform bulk solution. Because the surfactant is ionic, bulk phase transport is influenced by the electrical potential that develops at the interface due to accumulation of the specifically adsorbing, charged surfactant.

Simultaneous transport of three species is considered: a surface-active ion (e.g., dodecyl sulfate anions), its associated indifferent counterion (e.g., sodium cations), ad an indifferent co-ion (e.g., chloride anions) resulting from the addition of a background electrolyte species (e.g., NaCl) to the solution. All species are insoluble in the nonaqueous phase. As depicted schematically in Figure 1, ions within the potential field of the double layer, of thickness λ, experience electrostatic interaction with the charged surfactant-laden interface. Thus, indifferent counterions and co-ions within the double layer accumulate and are expelled, respectively. Surfactants very near the interface specifically adsorb, leading to a net transport of surfactant to the interface. However, the surfactant ions diffusing within the electrical double layer must overcome the electrostatic repulsion from the interface. Hence, the rate of transport of an ionic surfactant to the interface must be slower than that of an equivalent nonionic surfactant.

Transport Model. Transport of each charged species, i (where $i = 1$ is the surfactant ion, $i = 2$ is the counterion, and $i = 3$ is the co-ion), with valence z_i and diffusion coefficient D_i, under the influence of an electrical potential ψ, is described by the Nernst–Planck diffusion-migration equation:

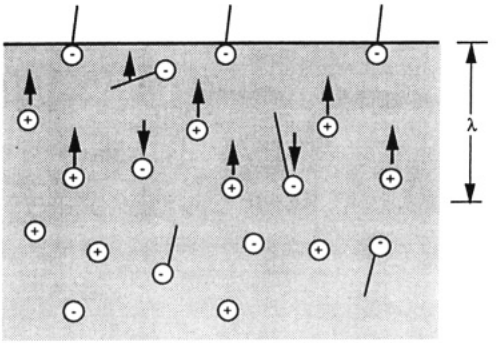

Figure 1. Schematic of ionic surfactant transport to a fluid/fluid interface. Negatively charged surfactant, represented by lined circles, specifically adsorbs on the interface, setting up an electrical double-layer field. Positively charged counterions accumulate within this double layer while negatively charged surfactant and negative co-ions are expelled.

$$\frac{\partial c_i}{\partial t} = D_i \frac{\partial}{\partial x}\left(\frac{\partial c_i}{\partial x} + z_i c_i \frac{F}{RT}\frac{\partial \psi}{\partial x}\right) \quad i = 1,2,3 \tag{1}$$

In this expression, c_i is the volume concentration of each species that depends on both time, t, and normal distance from the interface, x; F is the Faraday constant, R is the ideal gas constant, and T is absolute temperature. The electrical potential is related to the ion distribution through Poisson's equation:

$$\frac{\partial^2 \psi}{\partial x^2} = -\frac{F}{\epsilon}\sum_{i=1}^{3} z_i c_i \tag{2}$$

The initial condition and the boundary conditions far from the interface are obtained by assuming uniform initial concentration, no depletion of surfactant, and zero reference potential far from the interface:

$$c_i(x,0) = c_i^{\infty} \tag{3a}$$

$$c_i(\infty,t) = c_i^{\infty} \tag{3b}$$

$$\psi(x,0) = 0 \tag{3c}$$

$$\psi(\infty,t) = 0 \tag{3d}$$

A mass balance relating the surfactant specific adsorption at the interface, Γ_1^s, to the flux from the bulk,

$$\frac{d\Gamma_1^s}{dt} = D_1\left(\left.\frac{\partial c_1}{\partial x}\right|_{x=0} + z_1 c_1^s \frac{F}{RT}\left.\frac{\partial \psi}{\partial x}\right|_{x=0}\right) \tag{3e}$$

where c_1^s is the bulk concentration of surfactant at $x = 0$, along with no specific adsorption of counterions or co-ions,

$$\left.\frac{\partial c_i}{\partial x}\right|_{x=0} + z_i c_i^s \frac{F}{RT}\left.\frac{\partial \psi}{\partial x}\right|_{x=0} = 0 \quad i = 2, 3 \tag{3f}$$

gives the concentration boundary conditions at the interface. Finally, since the total surface charge is proportional to both the gradient in potential and the surfactant adsorption,[24] the final boundary condition is

(22) Borwanker, R. P.; Wasan, D. T. *Chem. Eng. Sci.* **1988**, *43*, 1323.
(23) Murphey, W. D.; Manzanares, J. A.; Mafe, S.; Reiss, H. *J. Phys. Chem.* **1992**, *96*, 9983.
(24) Newman, J. *Electrochemical Systems*, 2nd ed.; Prentice-Hall: Englewood Cliffs, NJ, 1991.

given by

$$\left.\frac{\partial\psi}{\partial x}\right|_{x=0} = -z_1\frac{F}{\epsilon}\Gamma_1^s \tag{3g}$$

where ϵ is the dielectric permittivity of the solvent. In addition to the specific adsorption at the interface, the total amount of surfactant adsorbed includes a small (negative) nonspecific contribution from the electrical double layer. Also, as a first approximation, we neglect the presence of a Stern layer and any specific counterion binding to the adsorbed surfactant.

Solution of eqs 1 and 2 subject to boundary conditions of eqs 3 requires a constitutive equation relating the bulk concentration of surfactant anions adjacent to the interface, c_1^s, to the adsorption of surfactant on the interface. In the case of diffusion-limited transport, a local equilibrium expression is demanded. In the more general case, where kinetic limitations to surfactant exchange between the bulk and interface occur, a kinetic constitutive equation is necessary. Here, we adopt a Frumkin equilibrium isotherm, extended to account for a charged surfactant,

$$\Gamma_1^s = \frac{Kc_1^s\Gamma_m}{Kc_1^s + \exp\left(\omega\frac{\Gamma_1^s}{\Gamma_m}\right)} \tag{4}$$

and correspondingly, Frumkin kinetics,

$$\frac{d\Gamma_1^s}{dt} = k_{-1}\left(Kc_1^s(\Gamma_m - \Gamma_1^s) - \Gamma_1^s\exp\left(\omega\frac{\Gamma_1^s}{\Gamma_m}\right)\right) \tag{5}$$

as mass transfer constitutive equations. Note that electrostatic effects appear implicitly in eqs 4 and 5 through the sublayer concentration, c_1^s. At equilibrium when $c_1^s = c_1^\infty \exp(-z_1\phi^s)$, where ϕ^s is the potential at the interface, and when $\omega = 0$, the Frumkin model of eq 4 reduces to the Davies isotherm for ionic surfactant adsorption.[20,21] Hence, the adsorption equilibrium constant, K, maximum surfactant adsorption, Γ_m, and surfactant lateral interaction parameter, ω, are found from equilibrium surface tension measurements. The rate constant for surfactant desorption, k_{-1}, reflects the rate of local surfactant exchange between the interface and bulk.

Examination of eqs 1–3 reveals that transient ionic surfactant transport to an interface is simply a more general case of the Ward–Tordai analysis for noncharged adsorbing species. In the case of uncharged surfactants, the valences and electrostatic potential are zero, and eqs 1 and 3 lead to the classical Ward–Tordai equations for adsorbing species and to a constant bulk concentration for any nonadsorbing species. Further, eqs 1–3 apply whether or not the electrical double-layer potential is in instantaneous equilibrium with the interface. Thus, the proposed ionic surfactant model encompasses the quasi-equilibrium double-layer models derived previously[1-4] but is not subject to the restriction of equilibrium concentrations and/or potential in the double layer. We also note that the model is applied with equal ease to surfactants of any valence and for any values of the ionic species diffusion coefficients, or indeed to solid/liquid interfaces that may bare a nascent charge prior to surfactant adsorption (with suitable modification of eq 3g). In addition, with appropriate alteration of the interfacial species mass balance (i.e., eq 3e) and constitutive equations (i.e., eqs 4 and 5), the model is easily extended to consider species soluble in the second phase and multiple surface-active species.

To facilitate numerical solution, the transport equations are nondimensionalized. We recognize two relevant length (and time) scales: the Debye length, $\lambda \equiv (\epsilon RT/F^2\bar{c})^{1/2}$, where $\bar{c} \equiv \sum_{i=1}^{3} z_i^2 c_1^\infty$, which gauges the electrical double-layer thickness, and the adsorption layer thickness, Γ_m/c_1^∞, which corresponds to the characteristic distance over which surfactant concentration changes occur in the bulk solution during the adsorption process. To examine electrostatic effects on surfactant transport, it is useful to compare the transient adsorption of an ionic surfactant to an equivalent nonionic surfactant. Thus, we adopt the adsorption length for scaling, since it is the only relevant length scale for nonionic surfactants. We employ c_1^∞ as the appropriate concentration for scaling the surfactant ion concentration. However, since the bulk counterion concentration and ionic strength are always of the same order (i.e., $c_2^\infty = O(\bar{c})$), and since the effect of background electrolyte on ionic surfactant transport only becomes important when $c_3^\infty \geq c_1^\infty$ (i.e., $c_3^\infty = O(\bar{c})$), $\bar{c}$ scales both counterion and co-ion concentrations. Accordingly, we define the following dimensionless variables:

$$\xi \equiv xc_1^\infty/\Gamma_m$$

$$\tau \equiv tD_1(c_1^\infty/\Gamma_m)^2$$

$$\phi \equiv \psi F/RT$$

$$C_1 \equiv c_1/c_1^\infty$$

$$C_i \equiv c_i/\bar{c} \quad i = 2,3$$

$$\theta \equiv \Gamma_1^s/\Gamma_m \tag{6}$$

With these variables eqs 1 and 2 become

$$\frac{\partial C_i}{\partial\tau} = \frac{D_i}{D_1}\frac{\partial}{\partial\xi}\left(\frac{\partial C_i}{\partial\xi} + z_iC_i\frac{\partial\phi}{\partial\xi}\right) \quad i = 1, 2, 3 \tag{7}$$

and

$$\frac{\partial^2\phi}{\partial\xi^2} = -\left(\frac{\Gamma_m}{c_1^\infty\lambda_1}\right)^2\left(z_1C_1 + z_2\frac{\bar{c}}{c_1^\infty}C_2 + z_3\frac{\bar{c}}{c_1^\infty}C_3\right) \tag{8}$$

where $\lambda_1 \equiv (\epsilon RT/F^2c_1^\infty)^{1/2}$ is a Debye length based solely on the surfactant ion concentration. The boundary conditions of eqs 3 become

$$C_1(\xi,0) = 1,\ C_i(\xi,0) = C_i^\infty \quad i = 2,3 \tag{9a}$$

$$C_1(\infty,\tau) = 1,\ C_i(\infty,\tau) = C_i^\infty \quad i = 2,3 \tag{9b}$$

$$\phi(\xi,0) = 0 \tag{9c}$$

$$\phi(\infty,\tau) = 0 \tag{9d}$$

$$\frac{d\theta}{d\tau} = \left.\frac{\partial C_1}{\partial\xi}\right|_{\xi=0} + z_1C_1^s\left.\frac{\partial\phi}{\partial\xi}\right|_{\xi=0} = \frac{k_{-1}}{D_1}\left(\frac{\Gamma_m}{c_1^\infty}\right)^2[\kappa C_1^s(1-\theta) - \theta\exp(\omega\theta)] \tag{9e}$$

$$\left.\frac{\partial C_i}{\partial\xi}\right|_{\xi=0} + z_iC_i^s\left.\frac{\partial\phi}{\partial\xi}\right|_{\xi=0} = 0 \quad i = 2,3 \tag{9f}$$

$$\left.\frac{\partial\phi}{\partial\xi}\right|_{\xi=0} = -z_1\left(\frac{\Gamma_m}{c_1^\infty\lambda_1}\right)^2\theta \tag{9g}$$

Several dimensionless groups appear in eqs 7–9. The

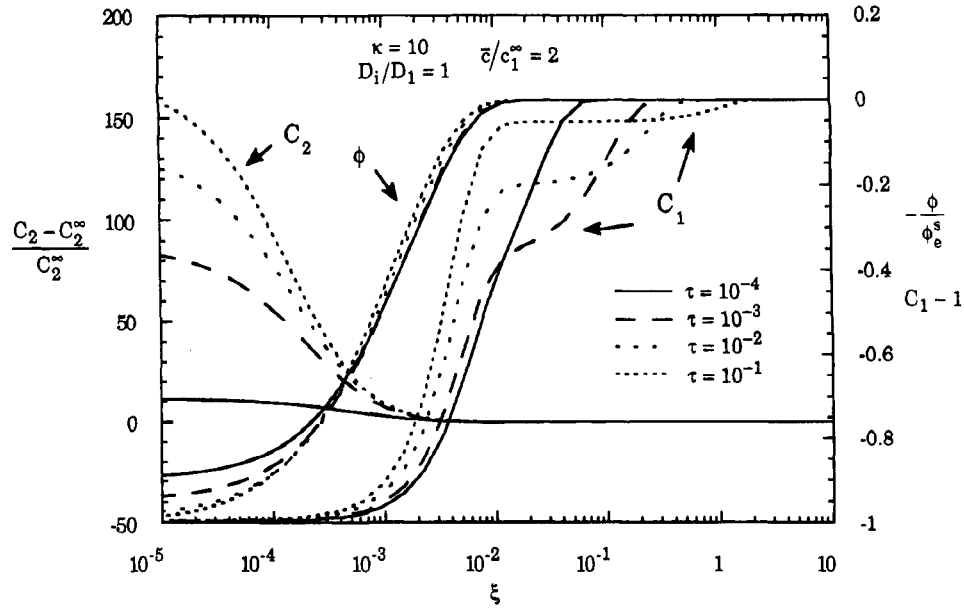

Figure 2. Concentration and potential profiles for diffusion-limited transport of a weakly adsorbing 1:1 ionic surfactant. Parameters: $\kappa = 10$, $\omega = 0$, $\bar{c}/c_1^\infty = 2$, $\Gamma_m/c_1^\infty\lambda_1 = 350$, $D_i/D_1 = 1$.

parameters $\kappa = Kc_1^\infty$ and ω from the Frumkin isotherm relate how strongly individual surfactant molecules adsorb at the interface and how strongly adsorbed surfactants interact laterally within the interface, respectively. The ratio of the kinetic rate constant to the diffusion rate $k_{-1}(\Gamma_m/\sqrt{D_1}c_1^\infty)^2$ determines whether kinetic or diffusion resistances control the rate of adsorption at the interface. For all calculations in this work, this parameter is set sufficiently high (i.e., $k_{-1}(\Gamma_m/\sqrt{D_1}c_1^\infty)^2 > 10^6$) to ensure that diffusion-limited transport occurs for all times probed (i.e., $\tau > 10^{-4}$). Whenever diffusion of multiple species is considered, ratios of diffusion coefficients are characteristic parameters. For transport of an ionic surfactant in the presence of background electrolyte, the ratio of the ionic strength to the surfactant concentration, $\bar{c}/c_1^\infty$, determines whether surfactant in the electrical double layer contributes significantly to the electric field.

The final dimensionless group, $\Gamma_m/c_1^\infty\lambda_1$, is the ratio of adsorption thickness to the Debye length based only on surfactant concentration. The maximum coverage for many commonly used ionic surfactants is nearly the same, so in these cases $\Gamma_m/c_1^\infty\lambda_1$ is primarily a function of surfactant concentration. At equilibrium, $\Gamma_1^s/\bar{c}\lambda = 2z_1 \sinh(\phi^s/2)$ for a symmetric surfactant–counterion pair. Accordingly, since Γ_m is the maximum value of Γ_1^s, and $(\sqrt{2}|z_1|)c_1^\infty\lambda_1$ is the minimum value of $\bar{c}\lambda$ for a symmetric surfactant with no background electrolyte present, $\Gamma_m/c_1^\infty\lambda_1$ gives an indication of maximum surface potential for a given surfactant concentration. Accordingly, this parameter determines the maximum effect of charge on both equilibrium and transient adsorption for a given surfactant concentration.

Equations 7–9 are solved numerically using finite differences, following the procedure of Murphey et al.[23,25] We use a centered differencing scheme on a nonuniform grid for the spatial domain. The resulting set of coupled nonlinear ODEs is solved using Gear's predictor–corrector integration method[26] for stiff systems, as implemented by the program LSODI.[27]

(25) MacLeod, C. A. Ph.D. Thesis, University of California, Berkeley, 1994.

Results

Figure 2 shows concentration profiles of surfactant and counterions, and electrostatic potential profiles for diffusion-limited transport of a 1:1 surfactant with no background electrolyte present (i.e., $\bar{c}/c_1^\infty = 2$). The surfactant is weakly adsorbing with $\kappa = 10$. Concentrations are plotted as $(C_i - C_i^\infty)/C_i^\infty$, so zero corresponds to the bulk concentration, negative numbers correspond to concentrations less than the bulk, and positive numbers correspond to concentrations greater than the bulk. The potential is plotted as $-\phi/\phi_e^s$, where ϕ_e^s is the equilibrium surface potential. All profiles are graphed on a semilogarithmic scale, for several values of τ approaching equilibrium.

In Figure 2, the distance over which the electrical potential magnitude decays to zero defines the electrical double-layer thickness. Within the double layer, counterion accumulation (species 2) increases with time to neutralize the increasing interfacial charge. The distance over which the surfactant concentration, C_1, reaches the bulk concentration defines the diffusion boundary layer thickness. For $\tau \leq 10^{-4}$, the surfactant concentration at the double-layer outer boundary is low, and the diffusion boundary layer extends only somewhat farther from the interface than the double layer (i.e., less than a factor of 10). With increasing τ, the concentration at the outer double-layer boundary increases as surfactant transports to the interface. Correspondingly, the diffusion boundary layer thickness increases. By $\tau = 10^{-2}$ the diffusion layer grows significantly larger than the double layer, and there is a distinct separation between the diffusion boundary layer and the electric double layer. By around $\tau = 1$, equilibrium (i.e., $C_1 = 1$ everywhere outside the double layer) is established.

Figure 3 shows similar profiles for a 1:1 surfactant with a 1:1 background electrolyte present at 100 times the surfactant concentration (i.e., $\bar{c}/c_1^\infty = 202$). In this case, the electric double-layer thickness is around an order of magnitude smaller than the no added salt case of Figure 2. Here equilibrium is not reached until around $\tau = 10$.

(26) Gear, C. W. *Numerical Initial Value Problems in Ordinary Differential Equations*; Prentice Hall: Old Tappan, NJ, 1971.
(27) Hindmarsh, A. C. *ACM SIGNUM Newslett.* **1980**, *15*, 10.

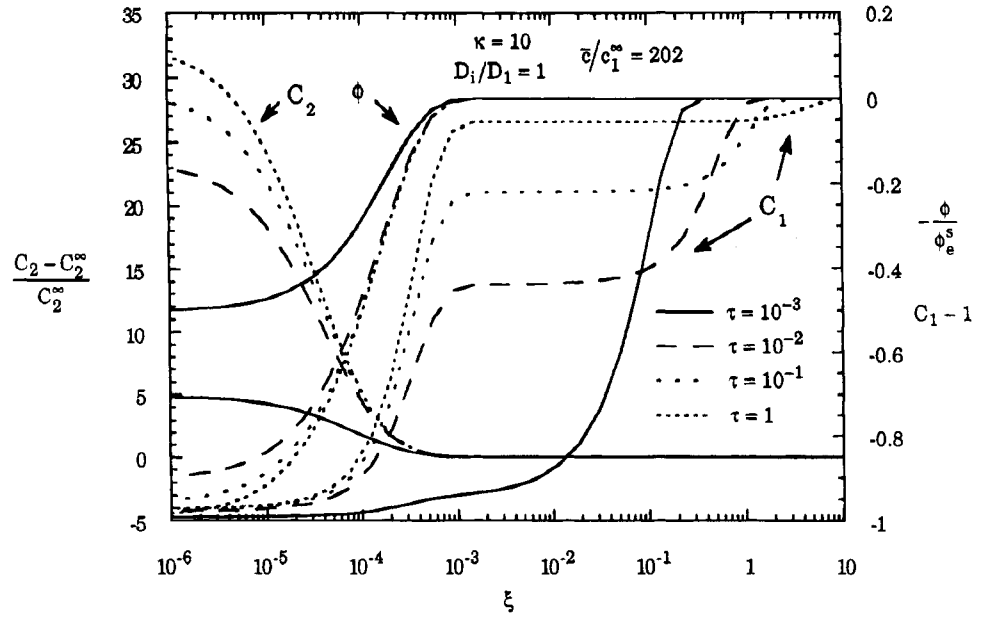

Figure 3. Concentration and potential profiles for diffusion-limited transport of a weakly adsorbing 1:1 ionic surfactant in the presence of a 1:1 background electrolyte at 100 times the surfactant concentration. Parameters: $\kappa = 10$, $\omega = 0$, $\bar{c}/c_1^\infty = 202$, $\Gamma_m/c_1^\infty\lambda_1 = 350$, $D_i/D_1 = 1$.

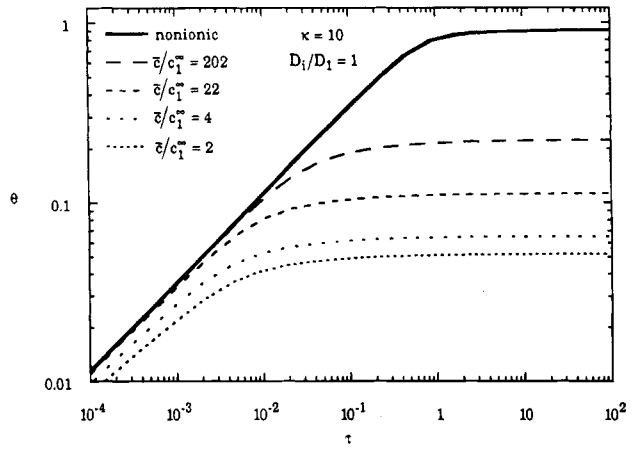

Figure 4. Diffusion-limited transient specific adsorption of a weakly adsorbing 1:1 ionic surfactant. Different curves correspond to different amounts of added 1:1 background electrolyte. The upper curve is for a nonionic surfactant. Parameters: $\kappa = 10$, $\omega = 0$, $\Gamma_m/c_1^\infty\lambda_1 = 350$, $D_i/D_1 = 1$.

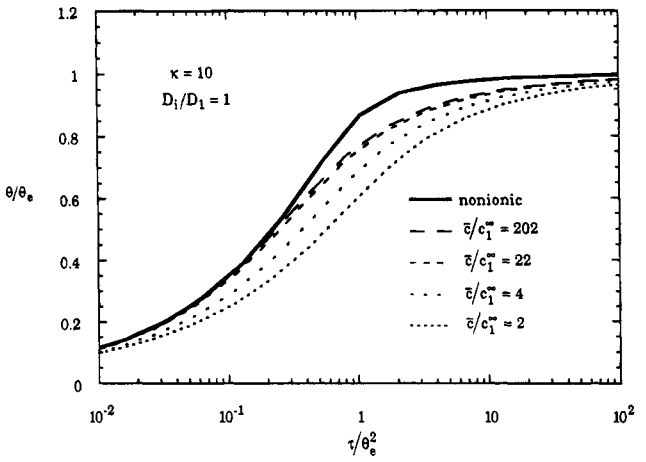

Figure 5. Diffusion-limited transient specific adsorption of a weakly adsorbing 1:1 ionic surfactant. Different curves correspond to different amounts of 1:1 background electrolyte. Results are scaled to account for differences in equilibrium coverages. The upper curve is for a nonionic surfactant. Parameters: $\kappa = 10$, $\omega = 0$, $\Gamma_m/c_1^\infty\lambda_1 = 350$, $D_i/D_1 = 1$.

However, even as early as $\tau = 10^{-3}$, a clear separation occurs between the electrical double layer and the diffusion boundary layer.

The profiles in Figures 2 and 3 show the responses of various species to the buildup of interfacial charge. However, ultimately we are interested in the transient adsorption at the interface and the differences between ionic and nonionic surfactant adsorption kinetics. Figure 4 plots surfactant-specific adsorption versus time for an ionic surfactant with varying amounts of background electrolyte. The dark solid line bounding the ionic surfactant results reflects the transient adsorption obtained for a nonionic surfactant using the standard Ward–Tordai diffusion analysis with a Langmuir isotherm (i.e., $\omega = 0$ in eq 4). As expected, electrostatic repulsion between adsorbed surfactants decreases the equilibrium coverage of an ionic surfactant relative to a nonionic surfactant with the same tendency to adsorb (i.e., with the same value of κ). While the nonionic surfactant reaches a high equilibrium coverage, $\theta_e = 0.9$, the ionic surfactant equilibrium coverages are much lower, ranging from around $\theta_e = 0.05$ with no added electrolyte to around $\theta_e = 0.22$ with background electrolyte present at 100 times the surfactant concentration. Lower equilibrium coverages naturally lead to shorter times to establish equilibrium. Hence, it is difficult to determine from Figure 4 the effect that electrostatic charge has on the rate of transport of an ionic surfactant, compared to that due solely to changes in equilibrium coverage.

To gain a clearer picture of charge effects on surfactant transport, we replot the data of Figure 4 in a manner that negates the differences that are purely due to changes in equilibrium coverage. Figure 5 plots the surfactant-specific adsorption divided by the equilibrium adsorption (i.e., θ/θ_e) versus time nondimensionalized by the equilibrium adsorption rather than the maximum adsorption (i.e., $\tau/\theta_e^2 = tD_1(c_1^\infty/\Gamma_{1e}^s)^2$). As expected, the transport of an ionic surfactant to the charging interface is slower than the transport of an equivalent nonionic surfactant. With no added electrolyte, the adsorption reaches 90% of its equilibrium value at $\tau/\theta_e^2 = 10$. This is a factor of 10 larger than the value of $\tau/\theta_e^2 = 1$, where the nonionic

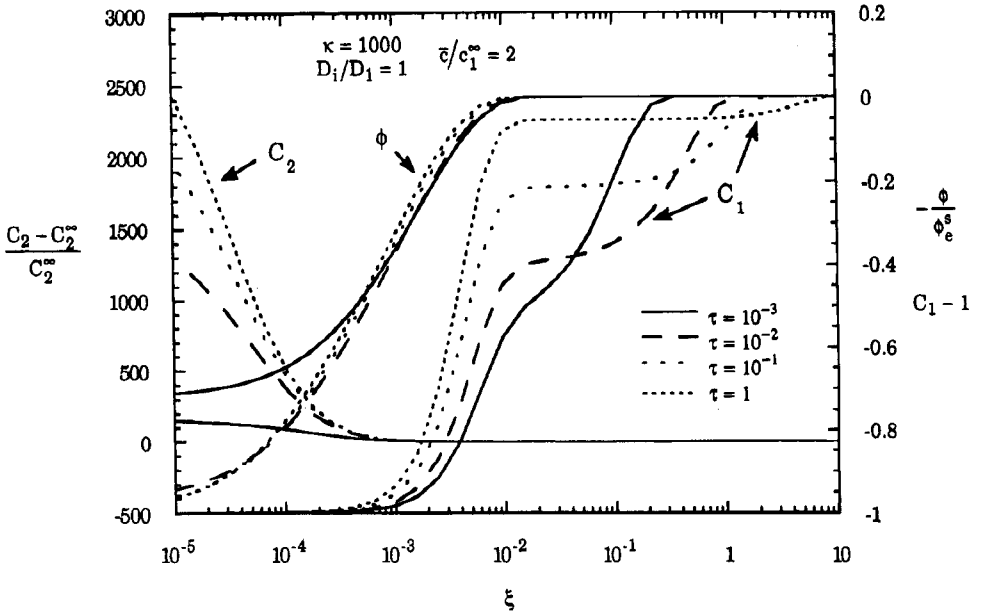

Figure 6. Concentration and potential profiles for diffusion-limited transport of a strongly adsorbing 1:1 ionic surfactant. Parameters: $\kappa = 1000$, $\omega = 0$, $\bar{c}/c_1^\infty = 2$, $\Gamma_m/c_1^\infty\lambda_1 = 350$, $D_i/D_1 = 1$.

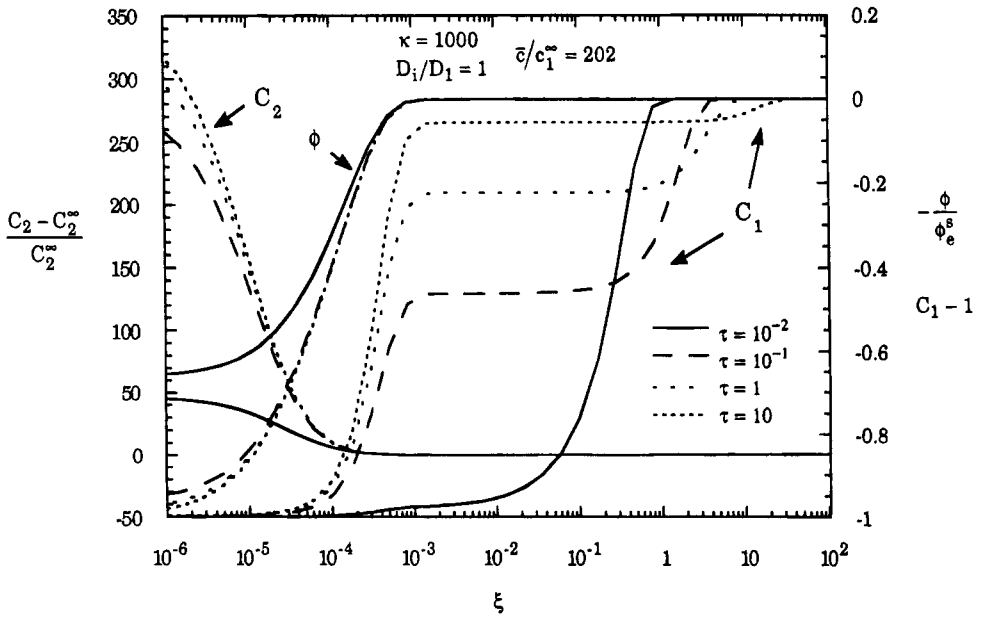

Figure 7. Concentration and potential profiles for diffusion-limited transport of a strongly adsorbing 1:1 ionic surfactant in the presence of 1:1 background electrolyte at 100 times the surfactant concentration. Parameters: $\kappa = 1000$, $\omega = 0$, $\bar{c}/c_1^\infty = 202$, $\Gamma_m/c_1^\infty\lambda_1 = 350$, $D_i/D_1 = 1$.

surfactant reaches 90% of equilibrium coverage. As background electrolyte is added, the electrical double layer is reduced in size relative to the adsorption layer, and the overall effect of charge on surfactant transport is reduced. In the case of $\bar{c}/c_1^\infty = 202$, the dimensionless time needed to reach 90% of equilibrium coverage is only a factor of 2 larger than that for a nonionic surfactant. Thus, adding background electrolyte decreases the effect that electrostatic repulsion has on surfactant transport.

Results in Figures 2–5 correspond to a weakly adsorbing surfactant or to very low surfactant concentration. Significant lowering of the surface tension from the pure solvent value occurs only for higher values of κ. Figures 6 and 7 show concentration and potential profiles for a more typical value of $\kappa = 1000$. In Figure 6 data are plotted for the case where no background electrolyte is present, and in Figure 7 data are plotted for background electrolyte present at 100 times the surfactant concentration. These profiles are very similar to those of Figures 2 and 3. The main difference is that for $\kappa = 1000$ the equilibrium adsorption is higher, requiring surfactants to diffuse from a larger distance in the bulk solution. Thus, the clear distinction between the electrical double layer and the diffusion boundary layer occurs for smaller τ and lower background electrolyte concentrations than for $\kappa = 10$.

Figure 8 presents calculations for the transient adsorption of surfactant on the interface when $\kappa = 1000$. As in Figure 5, the axes in Figure 8 are rescaled to account for differences in equilibrium coverages, with the equilibrium coverage for each curve indicated in the figure inset. Equilibrium coverages for the ionic surfactant increase significantly for all background electrolyte concentrations, compared to the weakly adsorbing surfactant of Figure 4. Conversely, the nonionic surfactant coverage, which was already high in Figure 4, shows only a small increase. Thus, differences in equilibrium surfactant adsorption,

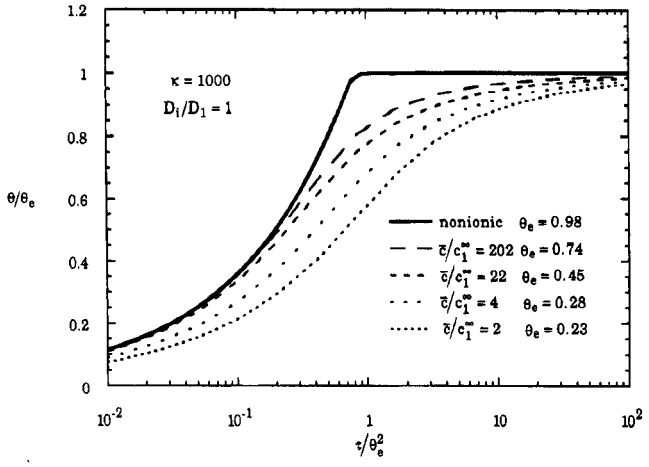

Figure 8. Diffusion-limited transient specific adsorption of a strongly adsorbing 1:1 ionic surfactant. Different curves correspond to different amounts of 1:1 background electrolyte. Results are scaled to account for differences in equilibrium coverages. The upper curve is for a nonionic surfactant. Parameters: $\kappa = 1000$, $\omega = 0$, $\Gamma_m/c_1^\infty\lambda_1 = 350$, $D_i/D_1 = 1$.

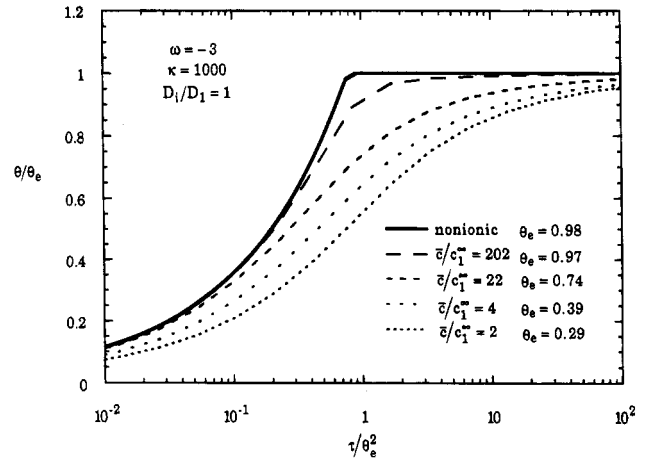

Figure 9. Diffusion-limited transient specific adsorption of a ionic surfactant with strong lateral interaction at the interface. Different curves correspond to different amounts of 1:1 background electrolyte. Results are scaled to account for differences in equilibrium coverages. The upper curve is for a nonionic surfactant. Parameters: $\kappa = 1000$, $\omega = -3$, $\Gamma_m/c_1^\infty\lambda_1 = 350$, $D_i/D_1 = 1$.

between an ionic and nonionic surfactant, are less pronounced for strongly adsorbing surfactants.

The transient adsorptions of Figure 8 show a more pronounced difference between ionic and nonionic surfactant adsorption dynamics than in Figure 5. When no background electrolyte is present, the dimensionless time for a strongly adsorbing surfactant to reach 90% of equilibrium adsorption is more than an order of magnitude greater than for a nonionic surfactant. Since surface charge is directly proportional to surfactant-specific adsorption, slower transport of the more strongly adsorbing surfactant is due to the stronger electrostatic repulsion the surfactant feels from the more highly charged interface.

The role of the surfactant lateral interaction on the transient adsorption of an ionic surfactant is shown in Figure 9, which again plots θ/θ_e versus τ/θ_e^2 for a strongly interacting surfactant with $\omega = -3$. At all ionic strengths, the equilibrium coverage increases as lateral interaction between surfactants increases. This effect is most pronounced at higher ionic strengths where the surfactant interfacial adsorption is greatest. Figure 9 shows that,

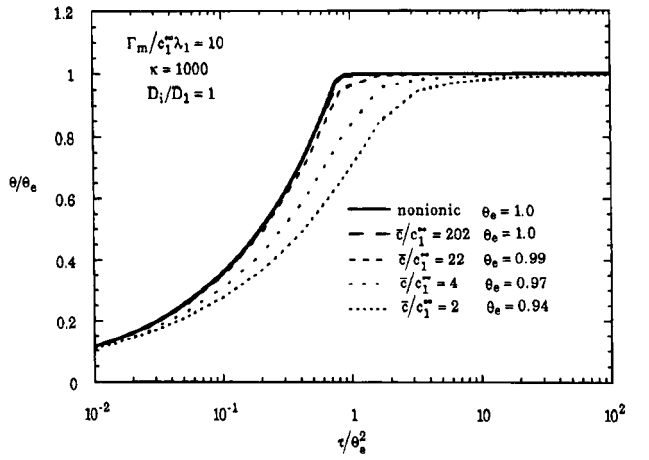

Figure 10. Diffusion-limited transient specific adsorption of a 1:1 ionic surfactant at high bulk concentration (or low maximum coverage). Different curves correspond to different amounts of 1:1 background electrolyte. Results are scaled to account for differences in equilibrium coverages. The upper curve is for a nonionic surfactant. Parameters: $\kappa = 1000$, $\omega = 0$, $\Gamma_m/c_1^\infty\lambda_1 = 10$, $D_i/D_1 = 1$.

for $\bar{c}/c_1^\infty \leq 22$, the increase in surfactant coverage (i.e., interfacial charge) slows down surfactant transport slightly as compared to Figure 8 where $\omega = 0$. Conversely, for $\bar{c}/c_1^\infty \geq 202$, surfactant coverage is high enough that attractive interactions between surfactants dominate over electrostatic repulsion, and the rate of surfactant transport to the interface actually increases over that in Figure 8.

As mentioned previously, the parameter $\Gamma_m/c_1^\infty\lambda_1$ determines the maximum surface potential and, hence, the maximum effect that charge can have on the equilibrium and transient adsorption of an ionic surfactant. The plots of Figures 2–9 all reflect a typical value for an ionic surfactant, $\Gamma_m/c_1^\infty\lambda_1 = 350$. Figure 10 plots θ/θ_e versus τ/θ_e^2 for the case where $\Gamma_m/c_1^\infty\lambda_1 = 10$, corresponding to high surfactant concentration (or low maximum coverage). As expected, the differences between ionic and nonionic equilibrium adsorption are now very small. At low indifferent electrolyte concentrations (i.e., $\bar{c}/c_1^\infty \leq 22$), ionic surfactant transport is still slower than for a nonionic surfactant, but the effect is much less than that seen for Figure 8 where $\Gamma_m/c_1^\infty\lambda_1 = 350$. Further, at high indifferent electrolyte concentrations (i.e., $\bar{c}/c_1^\infty = 202$), all electrostatic effects on surfactant transport vanish.

Diffusion coefficients of the large surfactant ions and typical smaller counterions and co-ions are clearly different. Figure 11 illustrates adsorption rates when the diffusion coefficients of counterions and co-ions are 10 times that of the surface active ion, as well as the case of equal diffusion coefficients, as shown in Figure 8. Both the absence of background electrolyte and electrolyte present at 100 times the surfactant concentration are considered. Results for equal diffusion coefficients, as shown previously in Figure 8, are presented along with a case where the diffusion coefficients of counterions and co-ions are 10 times that of the surface-active ion. For the no added salt case, we observe an increase in the rate of surfactant transport with increasing counterion diffusion coefficient. Note that the effect of fast counterion diffusion does not compensate completely for the retardation of surfactant due to electrostatic repulsion. Conversely, with background electrolyte present, there is no difference between the transient adsorption for equal and unequal ion diffusivities.

The reason for the different effects of unequal ion diffusivities in the presence and absence of background

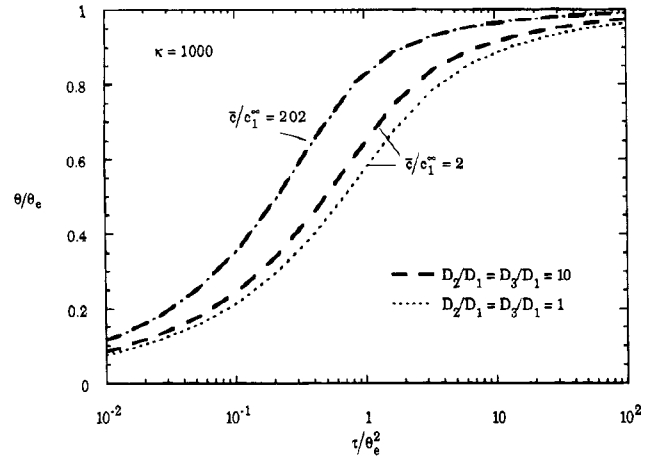

Figure 11. Diffusion-limited transient specific adsorption of a strongly adsorbing 1:1 ionic surfactant. Curves are shown comparing equal ion diffusion coefficients to a more realistic case where the counterion and co-ion diffusion coefficients are 10 times that of the surfactant ion diffusion coefficient. Results are shown for no background electrolyte and for 1:1 background electrolyte at 100 times the surfactant concentration. Parameters: $\kappa = 1000$, $\omega = 0$, $\Gamma_m/c_1^\infty\lambda_1 = 350$.

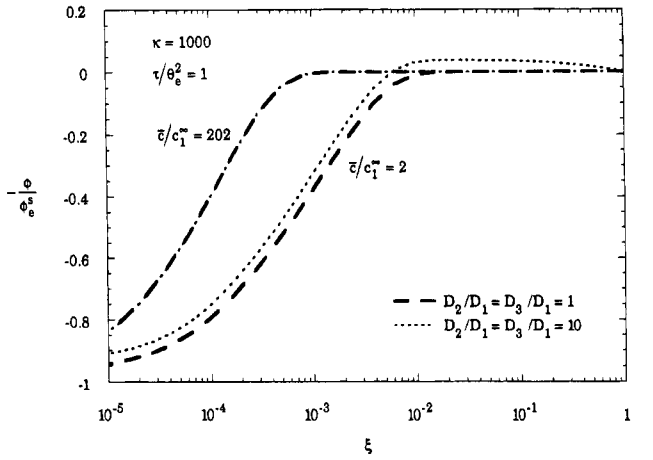

Figure 12. Potential profiles at $\tau/\theta_e^2 = 1$ for diffusion-limited transport of a strongly adsorbing 1:1 ionic surfactant with both equal and unequal ion diffusion coefficients. Results are for no background electrolyte and for 1:1 background electrolyte at 100 times the surfactant concentration. Parameters: $\kappa = 1000$, $\omega = 0$, $\Gamma_m/c_1^\infty\lambda_1 = 350$.

electrolyte is seen by examining the potential profiles corresponding to these cases. Figure 12 graphs the potential profiles at $\tau/\theta_e^2 = 1$ for equal and unequal ion diffusivities in both the presence and absence of background electrolyte. With no added salt and unequal diffusion coefficients, the potential is less negative and actually becomes positive outside of the electrical double layer. A migration potential is necessary to ensure that ionic species outside the double layer diffuse at the same rates to maintain electroneutrality everywhere in the bulk solution. Thus, the faster response of the counterions to the electrical potential in the double layer essentially drags along the more slowly diffusing surfactant anions. Observe from eq 8 that when $\bar{c}/c_1^\infty \gg 1$, the surfactant in the solution does not contribute significantly to the electric potential. Thus, with added electrolyte present, counterions and co-ions completely determine the potential profile. In this case, the migration potential is negligible, since the small indifferent ions have nearly the same diffusivities. Hence, surfactant transport is unaffected by the smaller ion diffusion rates.

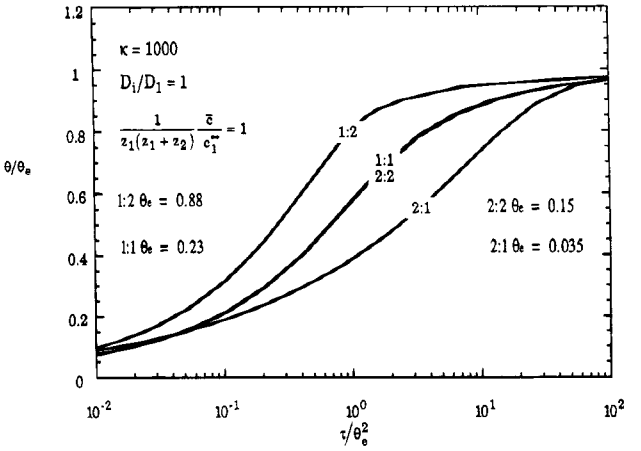

Figure 13. Diffusion-limited transient specific adsorption of a strongly adsorbing 1:1 ionic surfactant. Results are scaled to account for differences in equilibrium coverages. Curves are shown comparing symmetric 1:1 and 2:2 surfactant–counterion pairs to asymmetric 1:2 and 2:1 surfactant–counterion pairs. Results are for no background electrolyte. Parameters: $\kappa = 1000$, $\omega = 0$, $\Gamma_m/c_1^\infty\lambda_1 = 350$.

Dukhin et al. suggest that transport of multivalent surfactant species is affected more drastically than that of univalent surfactant species.[1,3] This hypothesis is easily checked using the general model presented here. Figure 13 displays transient and equilibrium adsorption for surfactant–counterion pairs of four different valence combinations with no added background electrolyte. Increasing the surfactant valence leads to greater repulsion between surfactants. Thus, the equilibrium coverage for a 2:1 surfactant–counterion pair is lower than that for a symmetric 1:1 pair. Conversely, increasing the counterion valence leads to greater screening of the surfactant charge. This enhanced screening allows a higher equilibrium coverage for a 1:2 surfactant ion–counterion pair than for a 1:1 pair. For the symmetric 2:2 surfactant ion–counterion pair, the effects of increased repulsion and increased screening nearly cancel, and the equilibrium coverage is only slightly lower than for the 1:1 pair.

The transient adsorptions of Figure 13 show that for the 2:2 pair the effects of increased repulsion between surfactants and increased screening by counterions on the rate of surfactant transport exactly offset. Hence, the rate of transport of symmetric surfactant ion–counterion pairs is unaffected by the ion valences. However, there is a substantial difference between the transport rates of symmetric and asymmetric surfactant–counterion pairs. For the 2:1 pair the greater repulsion between surfactants in the bulk and at the interface decreases the rate of surfactant transport to the interface by around a factor of 5 compared to the 1:1 and 2:2 pairs. Conversely, for the 1:2 pair the increased screening by the counterions leads to approximately a factor of 5 increase in the rate of surfactant transport to the interface.

Quasiequilibrium Model. The concentration profiles of Figures 3 and 7 display a distinct separation between surfactant transport in the electric double layer near the interface and surfactant transport through the bulk solution beyond the influence of the interfacial potential. This separation suggests that the model presented here can be simplified by treating separately the surfactant diffusion through the electrically neutral outer region and the transport in an equilibrium double-layer inner region. This idea is developed in detail by Dukhin et al.[1-3] with the assumption that the double-layer potential is always in an instantaneous "quasiequilibrium" with the concen-

tration at the double-layer boundary, but the surfactant concentration is not. Here we pursue this idea in a manner similar to that of Borwanker and Wasan,[4] with the further simplification that the inner double-layer region, including surfactant, is in a quasiequilibrium state.

For equal ion diffusivities outside the electrical double layer, and for equal counterion and co-ion diffusivities when $\bar{c}/c_1^\infty \gg 1$, eqs 1 and 2 reduce to those describing transport of a nonionic surfactant. Thus, the well-known analytic solutions for nonionic surfactant transport of the form

$$\Gamma_1^s = \frac{1}{2}\sqrt{\frac{D_1}{\pi}}\int_0^t \frac{(c_1^\infty - c_1^\lambda)}{\sqrt{t - t_0}}\,dt_0 \qquad (10)$$

can describe the diffusion of ionic surfactants between the bulk and double-layer boundary, where c_1^λ is the surfactant concentration at the double-layer boundary. Outside the double layer, the co-ion concentration remains constant and the counterion concentration is such that electroneutrality is maintained (i.e., $-z_2c_2 = z_1c_1 + z_3c_3$).

In treating the transport in the electrical double layer, it is informative to rescale eqs 1–3 with length and time scales appropriate to this region. We define the new dimensionless variables $\eta = x/\lambda$ and $\varrho = tD_1/\lambda^2$. When $\bar{c}/c_1^\infty \gg 1$, the electrostatic potential profile is independent of surfactant concentration and the approach of Dukhin et al.[1-3] seems quite reasonable. However, when there is no added electrolyte (i.e., $\bar{c}/c_1^\infty = 2$ for a 1:1 binary surfactant), the surfactant concentration profile in the double layer contributes strongly to the potential profile, and the approach of Dukhin et al. may be questionable.

Nondimensionlizing the interfacial boundary condition in eq 3e to give

$$\frac{d\theta}{d\varrho} = \frac{\lambda c_1^\infty}{\Gamma_m}\left(\left.\frac{\partial C_1}{\partial \eta}\right|_{\eta=0} + z_1 C_1^s \left.\frac{\partial \phi}{\partial \eta}\right|_{\eta=0}\right) \qquad (11)$$

suggests a transparent scheme for treating the double-layer region. When the Debye length is much smaller than the adsorption layer thickness (i.e., when $\lambda c_1^\infty/\Gamma_m \ll 1$) the rate of adsorption and, hence, the flux to the interface are negligible, as seen on the time scale of the double-layer formation. For this case, not only are the electrostatic potential and counterion and co-ion concentrations in a state of quasiequilibrium, but the surfactant concentration is as well. For a typical 1:1 surfactant–counterion pair at concentrations below the critical micelle concentration, $\lambda c_1^\infty/\Gamma_m$ ranges from 10^{-2} to 10^{-4} and $\bar{c}/c_1^\infty$ ranges from 2 to 202 as background 1:1 electrolyte concentration is increased from zero to 100 times the surfactant concentration. Low values of $\lambda c_1^\infty/\Gamma_m$ suggest that assuming quasiequilibrium in the entire electrical double layer (including surfactant) is limited to the same circumstances as those of the Dukhin et al. model (i.e., the presence of background electrolyte and at times greater than the characteristic time for double-layer formation, λ^2/D_1).

In contrast to the Dukhin et al. model, a quasiequilibrium model assuming equilibrium surfactant distribution in the double layer is quite easy to implement, especially for 1:1 electrolyte pairs with equal diffusion coefficients. Transient specific adsorption is obtained by simultaneously solving eq 10 (using standard numerical techniques),[17,28,29] with the modified Davies equilibrium isotherm relating the surfactant adsorption on the interface to the concentration at $x = \lambda$,[20,21]

$$\Gamma_1^s = \frac{Kc_1^\lambda \Gamma_m}{Kc_1^\lambda + \exp\left(\omega\dfrac{\Gamma_1^s}{\Gamma_m} + z_1\phi^s\right)} \qquad (12)$$

and the Gouy-Chapman result, relating the interfacial charge to interfacial potential:[24]

$$z_1\Gamma_1^s = 2\bar{c}\lambda \sinh\left(\frac{\phi^s}{2}\right) \qquad (13)$$

To match the outer diffusion region to the inner double-layer region, we choose $x = \lambda$ as the location of the double-layer periphery. Fortunately, the exact matching location is unimportant since our quasiequilibrium approximation is valid only when the double-layer thickness is very small relative to the diffusion layer thickness. Thus, the time for surfactant to move from $x = \lambda$ to $x = 0$ is insignificant relative to the time it takes to reach $x = \lambda$. Our proposed quasiequilibrium model is a modification of that of Borwanker and Wasan.[4] Whereas Borwanker and Wasan use equilibrium values of λ and $\bar{c}$ in eq 13, we calculate λ and $\bar{c}$ self-consistently from instantaneous concentrations at $x = \lambda$ in the electrically neutral bulk solution.

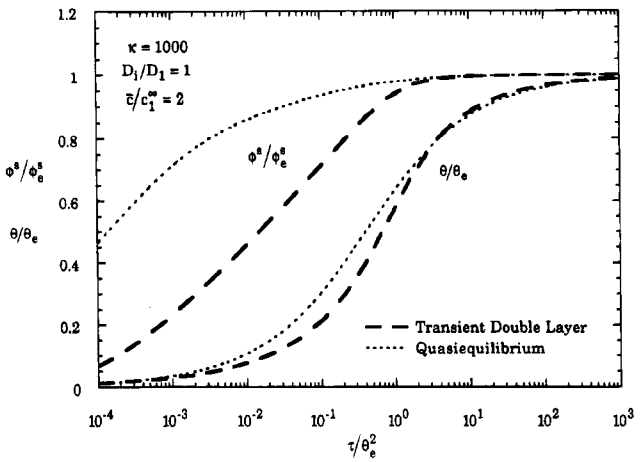

Figure 14. Diffusion-limited transient specific adsorption and potential for a strongly adsorbing 1:1 surfactant with no background electrolyte, $\bar{c}/c_1^\infty = 2$. Curves are shown comparing the full transient double-layer model to the quasiequilibrium model. Parameters: $\kappa = 1000$, $\omega = 0$, $\Gamma_m/c_1^\infty\lambda_1 = 350$, $D_i/D_1 = 1$.

Figures 14–16 compare the full transient double-layer model to our proposed quasiequilibrium model. Figure 14 plots transient specific adsorption and surface potential for the full and quasiequilibrium models for a strongly adsorbing 1:1 surfactant with no added electrolyte. As expected, the quasiequilibrium model predicts somewhat faster transport than the full model. Figures 15 and 16 show transient adsorptions and surface potentials for surfactant solution with increasing amounts of background electrolyte. Also as expected, the agreement between the quasiequilibrium and transient double-layer models becomes much better as the concentration of background electrolyte increases.

The usual method of validating models of surfactant transport to a fluid/fluid interface is by comparison to experimental dynamic surface tension data. The surface tension, σ, for an ionic surfactant in an indifferent electrolyte solution obeying an extended Davies equilibrium isotherm can be expressed as a function of the adsorption of surfactant on the interface and the surface

(28) Borwanker, R. P.; Wasan, D. T. *Chem. Eng. Sci.* **1983**, *38*, 1637.
(29) Miller, R. *Colloid Polym. Sci.* **1981**, *259*, 375.

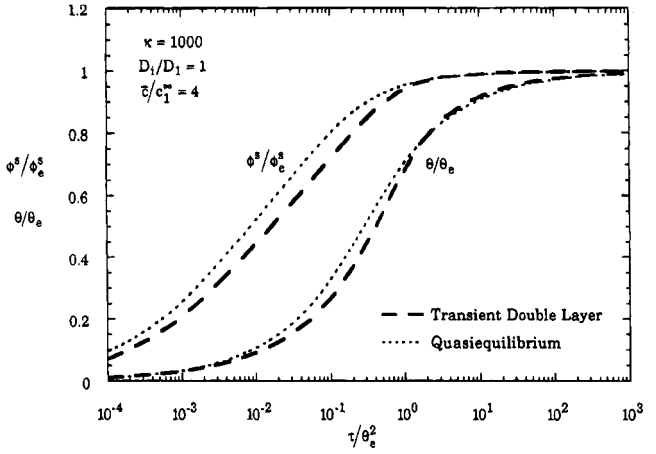

Figure 15. Diffusion-limited transient specific adsorption and potential for a strongly adsorbing 1:1 surfactant with an equal concentration background electrolyte, $\bar{c}/c_1^\infty = 4$. Curves are shown comparing the full transient double-layer model to the quasiequilibrium model. Parameters: $\kappa = 1000$, $\omega = 0$, $\Gamma_m/c_1^\infty\lambda_1 = 350$, $D_i/D_1 = 1$.

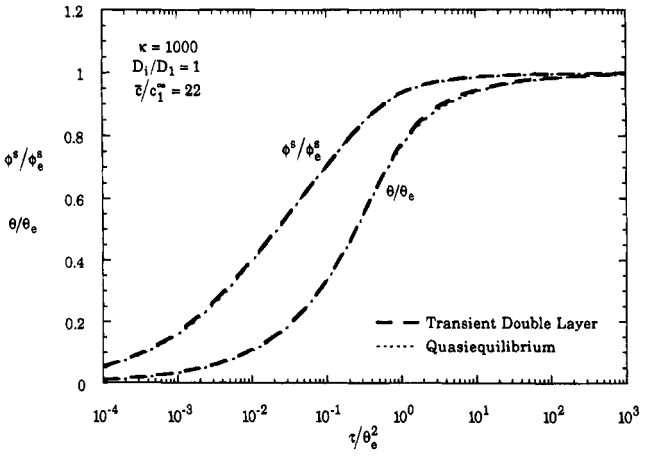

Figure 16. Diffusion-limited transient specific adsorption and potential for a strongly adsorbing 1:1 surfactant with background electrolyte at 10 times the surfactant concentration, $\bar{c}/c_1^\infty = 22$. Curves are shown comparing the full transient double-layer model to the quasiequilibrium model. Parameters: $\kappa = 1000$, $\omega = 0$, $\Gamma_m/c_1^\infty\lambda_1 = 350$, $D_i/D_1 = 1$.

potential:[22,30]

$$\sigma = \sigma_0 + RT\Gamma_m\left[\ln(1-\theta) - \frac{\omega}{2}\theta^2\right] - 4RT\bar{c}\lambda\left[\cosh\left(\frac{\phi^s}{2}\right) - 1\right] \quad (14)$$

where σ_0 is the tension of the surfactant-free electrolyte solution. Assuming that eq 14 holds during the transient adsorption process allows dynamic surface tensions to be calculated from the transient specific adsorptions and surface potentials such as in Figures 14–16. This calculation is straightforward for the quasiequilibrium model using the instantaneous surfactant-specific adsorption, the surface potential, and a local ionic strength and Debye length calculated from the instantaneous species concentrations at $x = \lambda$. When a dynamic surface tension is calculated with the full transient model, the species concentrations at the double-layer boundary are not as readily identified. Therefore, with the full model, we use eq 13 to calculate a pseudoionic strength (and Debye length) that corresponds to a hypothetical bulk solution in equilibrium with the interface. Since eqs 13 and 14 are derived using the Gouy–Chapman model of an equilibrium double layer, we recognize that this procedure for calculating surface tensions from the results of the full transient double-layer model is not rigorous.

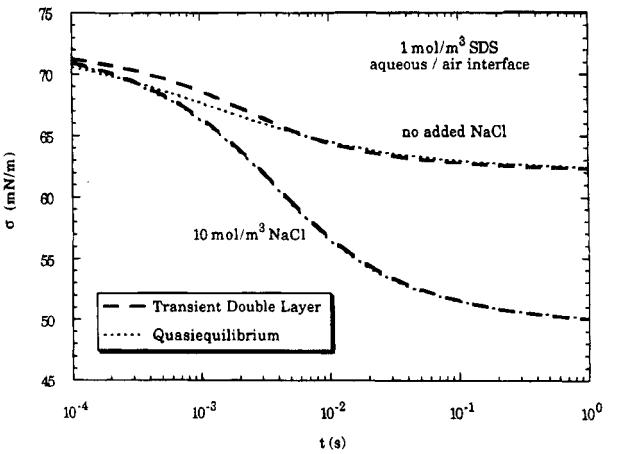

Figure 17. Calculated dynamic surface tension for 1 mol/m^3 sodium dodecyl sulfate with varying amounts of background sodium chloride. Results are presented for both the full transient adsorption model and the quasiequilibrium model. Parameters: $K = 680$ m^3/mol, $\omega = -0.65$, $\Gamma_m = 10^{-5}$ mol/m^2, $D_i = 6.65 \times 10^{-10}$ m^2/s.

Figure 17 presents calculated dynamic surface tensions for the aqueous 1 mol/m^3 SDS solution/air interface. Equilibrium parameters for SDS are obtained by fitting the data of Fainerman[12] using eq 14. Calculations using both the full transient double-layer model and the quasiequilibrium model are shown for two different background electrolyte concentrations. Our simple quasiequilibrium model does not allow for unequal ion diffusivities, so correspondingly, the transient model ion diffusivities are all assumed equal to the mean diffusion coefficient of SDS. As previously observed in Figure 14, there are differences between the results obtained with the two models at early times, particularly with no added electrolyte. However, we note that these discrepancies occur in a region that is seldom of interest because the surface tension is not lowered much from the pure solvent value. We also note that the times over which the two models differ is very short, on the order of 10^{-2} s, a time scale that is not accessible using most dynamic surface tension measurement techniques. The few techniques that are capable of measuring at such short times (e.g., the oscillating jet technique) have substantial surfactant mass transfer along the interface that is difficult to model.

Figure 17 also shows that ionic surfactant adsorption approaches equilibrium monotonically. There is no intermediate plateau in the dynamic tension arising from an electrostatic barrier and no partial accumulation of surfactant at the outer edge of the diffuse double layer before equilibrium is finally attained.[31] The transient surfactant concentration profiles in Figures 2, 3, 6, and 7 all indicate that the effects of charge on the interface are present almost instantaneously and that surfactant adsorption onto the charging interface monotonically slows.

Discussion

A rigorous model is outlined for ionic surfactant transport to an initially neutral, planar interface. Com-

(30) Davies, J. T.; Rideal, E. K. *Interfacial Phenomena*; Academic Press: New York, 1963.

(31) Bonfillon, A.; Sicoli, F.; Langevin, D. *J. Colloid Interface Sci.*, submitted for publication.

parison of model results for an ionic surfactant to results for an equivalent nonionic surfactant shows the importance of electrostatic effects. Neglecting electrostatics can lead to errors of more than an order of magnitude in predicted diffusion-limited equilibration times for low surfactant concentrations with no background electrolyte present. Clearly, any analysis of ionic surfactant dynamic surface tension measurements must account for such electrostatic interactions.

Given the numerical complexity of the full transient model, simpler models are desirable for describing ionic surfactant transport. Here we present one very simple model, assuming that the entire electrical double layer is in a state of quasiequilibrium with surfactant at the double-layer periphery. Comparison of this simple quasiequilibrium model to the more rigorous model for the commonly used surfactant SDS shows that the two models are equivalent over all times scales accessible via current dynamic surface tension measurements. Thus, for SDS (and surfactants with similar equilibrium partitioning at the interface), dynamic surface tension data interpreted by the quasiequilibrium model should provide information on whether transport is diffusion limited. However, our quasiequilibrium model neglects the effect of different surfactant and counterion diffusivities. To describe exactly the diffusion-limited transport of SDS over the range of electrolyte concentrations requires numerical calculation of an effective diffusion coefficient for SDS from the individual ion species diffusivities that will vary with background electrolyte concentration.[24]

We consider only a rather small range of adsorption parameters, so the conclusions obtained for SDS cannot be taken as universal. However, the two models developed here are easily compared for any identical valence surfactant ion:counterion:co-ion system, once the equilibrium adsorption parameters are known. For asymmetric electrolyte systems, analytic solutions for the Gouy–Chapman double-layer model are not possible. Thus, implementation of a quasiequilibrium model for an asymmetric electrolyte system requires numerical solution of the Gouy–Chapman double-layer model. Accordingly, for asymmetric systems much of the simplicity of the quasiequilibrium model is lost. In contrast, solution of the full transient double-layer model is unaffected by changing electrolyte valence.

One weakness of our transient double-layer model is that it ignores the finite size of ions in bulk solution and any specific counterion binding at the interface. Neglecting finite ion size allows the calculated concentration of counterions adjacent to the interface to exceed physically realizable values when the interface is highly charged and the Debye length is small. For typical parameter values of $\kappa = 1000$, $\omega = 0$, and $\Gamma_m/c_1^\infty\lambda_1 = 350$, we calculate counterion concentrations at the surface ranging from 2–30 kmol/m^3 as $\bar{c}/c_1^\infty$ increases from 2 to 202. Thus, at the highest background electrolyte concentrations, neglect of finite ion size is inappropriate. Fortunately, when finite ion size becomes important (i.e., high surfactant and background electrolyte concentration), electrostatic effects have a relatively minor impact on the transport of ionic surfactants. Thus, the error introduced by neglecting finite ion size is minimized.

With counterion binding at the interface, a fraction of the interfacial charge is neutralized by specific adsorption of counterions to the surfactant ion monolayer. The resulting reduction in interfacial potential diminishes electrostatic effects in ionic surfactant transport. Therefore, the model we present defines the maximum effect that charge has on ionic surfactant transport. As with finite ion size, counterion binding is most significant at high background electrolyte concentrations. Inclusion of more detailed electrostatic models into our transient double-layer calculation is certainly possible, requiring only modification of the boundary conditions.

Throughout this work, we focus on diffusion-limited surfactant transport and neglect possible finite adsorption kinetics. In our physical picture of ionic surfactant transport, a surfactant molecule that overcomes the electric field in arriving at the surface experiences the same electrical potential as an adsorbed surfactant. Thus, the kinetics of surfactant reorientation and adsorption onto the interface are not substantially different between ionic and nonionic surfactants of similiar sizes and shapes. For nonionic surfactants, kinetic limitations manifest at early times, while diffusion-limited transport occurs at later times when the diffusion boundary layer thickness has grown sufficiently large.[17] For ionic surfactants, charge accumulation on the interface slows the diffusion rate to the interface. Thus, the time scale for kinetic-limited transport to occur is shorter for an ionic surfactant than that for an equivalent nonionic surfactant.

Obviously, testing our transport model and determining whether ionic surfactant transport to the interface is diffusion-limited over a given time scale require experimental data. Currently, no suitable data for the dynamic surface tension of an ionic surfactant at varying background electrolyte concentrations exist to test our model. The required data must be obtained using a technique which fulfills the assumptions of the Ward–Tordai type of analysis (i.e., a stationary, planar interface with undisturbed underlying bulk fluid and an instantaneous, total depletion of surfactant at the interface at $t = 0$). Unfortunately, the techniques which meet these requirements (e.g., dynamic Whilhelmy plate or Du Nouy ring[6] or large pendant drops with negligible interfacial curvature)[13] are reliable only for times greater than a few seconds. Pure solutions of the commonly studied SDS show equilibration times of less than 1 s.[32] Thus, measurements on a more slowly adsorbing, pure surfactant are needed.

Conclusions

A rigorous model is presented to describe the diffusion-limited transport of ionic surfactants in a developing double-layer potential field. This model is valid over a wide range of electrolyte concentrations and applicable to surfactants, counterions, and co-ions of any valence and for any values of species diffusion coefficients. Although we have focused on fluid/fluid interfaces, the model applies to fluid/solid interfaces as well.

Comparison of this model to the Ward–Tordai analysis for nonionic surfactants reveals that the transport of ionic surfactant to the interface occurs significantly slower than the transport of a nonionic surfactant. Electrostatic effects are most profound for low concentrations of strongly adsorbing surfactant with no added background electrolyte in solution, where surfactant equilibration is slowed by more than an order of magnitude. With the addition of more surfactant or indifferent electrolyte, electrostatic effects decrease, and the transient adsorption of an ionic surfactant approaches that of a nonionic surfactant.

Calculations reveal substantial differences between the transport of asymmetric and symmetric surfactants with no added background electrolyte. Rates of surfactant transport to the interface for 1:1 and 2:2 surfactant ion–counterion pairs are identical. However, the rate of surfactant transport for a 1:2 pair is significantly higher

(32) Mysels, K. J. *Langmuir* **1986**, *2*, 423.

than for a symmetric pair. Conversely, the surfactant transport for a 2:1 pair is much lower than for a symmetric pair.

At low electrolyte concentrations, differences between counterion and surfactant ion diffusion coefficients influence the rate of surfactant transport to the interface. For the typical case, where the counterion diffusion coefficient is up to an order of magnitude larger than the surfactant ion diffusion coefficient, the surfactant transport rate is increased, but it remains slower than the nonionic transport rate. At high electrolyte concentrations, the counterion diffusion coefficient has no effect on the rate of surfactant transport.

We also propose a quasiequilibrium model to simplify the analysis of ionic surfactant transport. Compared to the rigorous transient double-layer model, this quasiequilibrium model is very easy to apply for symmetric electrolyte pairs with equal ion diffusivities. Comparison of this simple model to the transient double-layer model shows differences in transient adsorptions and potentials at early times and low background electrolyte concentrations. However, for a typical ionic surfactant, SDS, adsorbing at the air/water interface, these differences occur in a time domain that is experimentally inaccessible.

Acknowledgment. This work was partially supported by Grant CTS 9307890 of the Chemical and Thermal Systems Division—Interfacial Transport and Separation Processes Program of the National Science Foundation. Portions of this work were presented at the annual meeting of AIChE, St. Louis, MO (1993).

Nomenclature

c_i = concentration of species i, kmol/m^3
C_i = dimensionless concentration of species i
$\bar{c}$ = ionic strength, kmol/m^3
D_i = diffusion coefficient of species i, m^2/s
F = Faraday's constant, J/mol·V
k_{-1} = reverse rate constant for adsorption, s^{-1}
K = surfactant adsorption equilibrium constant, m^3/kmol
R = ideal gas constant, J/mol·K
t = time, s
T = temperature, K
x = normal distance from interface, m
z_i = valence of ionic species i

Greek Symbols

Γ_1^s = surfactant-specific adsorption at interface, kmol/m^2
Γ_m = maximum surfactant adsorption, kmol/m^2
ϵ = electric permittivity of solvent
η = dimensionless distance, x/λ
ϕ = dimensionless electrostatic potential
κ = parameter determining adsorption strength, Kc_1^∞
λ = Debye length, m
θ = dimensionless specific adsorption, Γ_1^s/Γ_m
ϱ = dimensionless double-layer time, D_1t/λ^2
σ = surface tension, N/m
σ_0 = surface tension of surfactant-free interface, N/m
τ = dimensionless adsorption layer time, $D_1t(c_1^\infty/\Gamma_m)^2$
ω = interfacial surfactant interaction parameter
ξ = dimensionless distance, xc_1^∞/Γ_m
ψ = electrostatic potential, V

Subscripts

e = equilibrium
i = ionic species
1 = surface-active ionic species
2 = counterion species
3 = co-ion species

Superscripts

s = evaluated adjacent to the interface
∞ = evaluated far from the interface
λ = evaluated at $x = \lambda$